

 Open access • Journal Article • DOI:10.1029/2019GL086115

## Urban Near-surface Seismic Monitoring using Distributed Acoustic Sensing

— [Source link](#) 

Gang Fang, Gang Fang, Yunyue Elita Li, Yumin Zhao ...+1 more authors

**Institutions:** National University of Singapore, Ministry of Land and Resources of the People's Republic of China, Virginia Tech

**Published on:** 28 Mar 2020 - Geophysical Research Letters (John Wiley & Sons, Ltd)

**Topics:** Distributed acoustic sensing and Passive seismic

Related papers:

- [Distributed Acoustic Sensing Using Dark Fiber for Near-Surface Characterization and Broadband Seismic Event Detection.](#)
- [Distributed Acoustic Sensing for Seismic Monitoring of The Near Surface: A Traffic-Noise Interferometry Case Study](#)
- [Dynamic strain determination using fibre-optic cables allows imaging of seismological and structural features](#)
- [Fiber-Optic Network Observations of Earthquake Wavefields](#)
- [Illuminating seafloor faults and ocean dynamics with dark fiber distributed acoustic sensing](#)

Share this paper:    

View more about this paper here: <https://typeset.io/papers/urban-near-surface-seismic-monitoring-using-distributed-5e93p9mn8g>

# Urban Near-surface Seismic Monitoring using Distributed Acoustic Sensing

Gang Fang<sup>1,2</sup>, Yunyue Elita Li<sup>1</sup>, Yumin Zhao<sup>1</sup>, and Eileen R. Martin<sup>3</sup>

<sup>1</sup>Department of Civil and Environmental Engineering, National University of Singapore, Singapore

<sup>2</sup>Key Laboratory of Marine Hydrocarbon Resources and Environmental Geology, Ministry of Land and  
Resources, Qingdao Institute of Marine Geology, Qingdao, 266071, China

<sup>3</sup>Department of Mathematics, Program in Computational Modeling and Data Analytics, Virginia Tech,  
Virginia, USA

## Key Points:

- Using the Stanford DAS array, we demonstrate the reliability of urban DAS recordings when deployed in existing infrastructures.
- Short DAS recordings of far-field quarry blasts show sensitivity to the changes in near-surface velocity within the boundaries of the array.
- DAS can play an important role in real time, high resolution, and long term urban monitoring applications.

---

Corresponding author: Yunyue Elita Li, [elita.li@nus.edu.sg](mailto:elita.li@nus.edu.sg)

## Abstract

Urban subsurface monitoring requires high temporal-spatial resolution, low maintenance cost, and minimal intrusion to nearby life. Distributed acoustic sensing (DAS), in contrast to conventional station-based sensing technology, has the potential to provide a passive seismic solution to urban monitoring requirements. Based on data recorded by the Stanford Fiber Optic Seismic Observatory, we demonstrate that near-surface velocity changes induced by the excavation of a basement construction can be monitored using existing fiber optic infrastructure in a noisy urban environment. To achieve the satisfactory results, careful signal processing comprising of noise removal and source signature normalization are applied to raw DAS recordings. Repeated blast signals from quarry sites provide free, unidirectional, and near-impulsive sources for periodic urban seismic monitoring, which are essential for increasing the temporal resolution of passive seismic methods. Our study suggests that DAS will likely play an important role in urban subsurface monitoring.

## 1 Plain Language Summary

Seismic monitoring can provide crucial information about near-surface changes due to natural or manmade activities. However, the high cost and the “after-effect” nature of conventional station-based monitoring methods limit their application in urban environments where near real-time and meter-scale resolution are required. Distributed acoustic sensing (DAS) has the potential to achieve all requirements utilizing existing communication infrastructure. Using Stanford Fiber Optic Seismic Observatory, we demonstrate that its recordings of quarry blasts 13.3 km away carry important subsurface velocity information within the footprint of the array. These short bursts of quarry blast signals provide us free, unidirectional, and repetitive sources that sample the urban subsurface at an interval frequent enough for monitoring. We observe large velocity decrease from the recordings close to the excavation site. Our study suggests that telecommunications fiber repurposed for DAS will potentially play an important role in many urban subsurface monitoring applications.

## 2 Introduction

Characterizing and monitoring changes in the top tens of meters of the Earth’s subsurface will play a significant role in satisfying the increasing need for urban sustainability and resilience (Díaz et al., 2017). Near-surface changes due to natural or man-made events may lead to hazards including ground subsidence (Tran & Sperry, 2018), sinkholes (Dahm et al., 2011; Gutiérrez et al., 2014), and landslides (Renalier et al., 2010; Schenato et al., 2017), which may result in direct casualties and damages to existing infrastructure (Douglas, 2004). Many such subsurface changes manifest themselves as temporal variations in geophysical properties (such as velocity, attenuation, electric conductivity, gravity, etc.) before catastrophic hazards occur, which can be monitored and predicted by geophysical prospecting.

Compared to conventional geophysical exploration for resources, near-surface monitoring in urban environments has unique acquisition requirements including high spatial resolution towards meter-scale, high temporal resolution towards real-time data collection and daily warning, low maintenance cost for long term monitoring and minimal intrusion to urban life. These requirements are met by a passive system enabled by DAS that we present in this paper. DAS arrays can measure strain along kilometers of optical fiber, producing large datasets with kilohertz time sampling and at sub-meter channel spacing (Parker et al., 2014). Over the past decade, DAS has been a rapidly evolving technology for downhole recording in oil and gas reservoirs (Willis et al., 2016). Recent success of DAS applications using existing telecommunication infrastructures (Jousset et al., 2018; Yu et al., 2019; Ajo-Franklin et al., 2019) demonstrates its cost-effectiveness

66 in deployment and maintenance. However, these experiments are conducted for appli-  
67 cations in earthquake seismology in remote areas where anthropogenic noise is rare and  
68 desired signals are clearly visible above the random noise in DAS measurements.

69 Studies using DAS arrays deployed in urban environments have reported that near-  
70 surface velocities can be estimated with ambient noise recorded by DAS over month-long  
71 periods (Dou et al., 2017; Martin et al., 2018; Spica et al., 2019). Averaging over long  
72 observation times is needed to suppress strong near-field anthropogenic noise, but severely  
73 limits the temporal resolution of passive seismic monitoring with DAS. Here we present  
74 a case study from the Stanford Fiber Optic Seismic Observatory where we take advan-  
75 tage of far-field anthropogenic activities - quarry blasts - to monitor the near-field an-  
76 thropogenic activity - excavation. Weekly quarry blasts can be used to sample the sub-  
77 surface with sufficient energy at intervals relevant to urban monitoring. We perform care-  
78 ful signal processing to reduce the effect of strong nearby noise and the variability in the  
79 blast sources. We demonstrate that with 100 seconds of DAS recordings after quarry blasts,  
80 near-surface velocity changes caused by construction of a basement within the array can  
81 be observed.

## 82 **3 Data and Signal Processing**

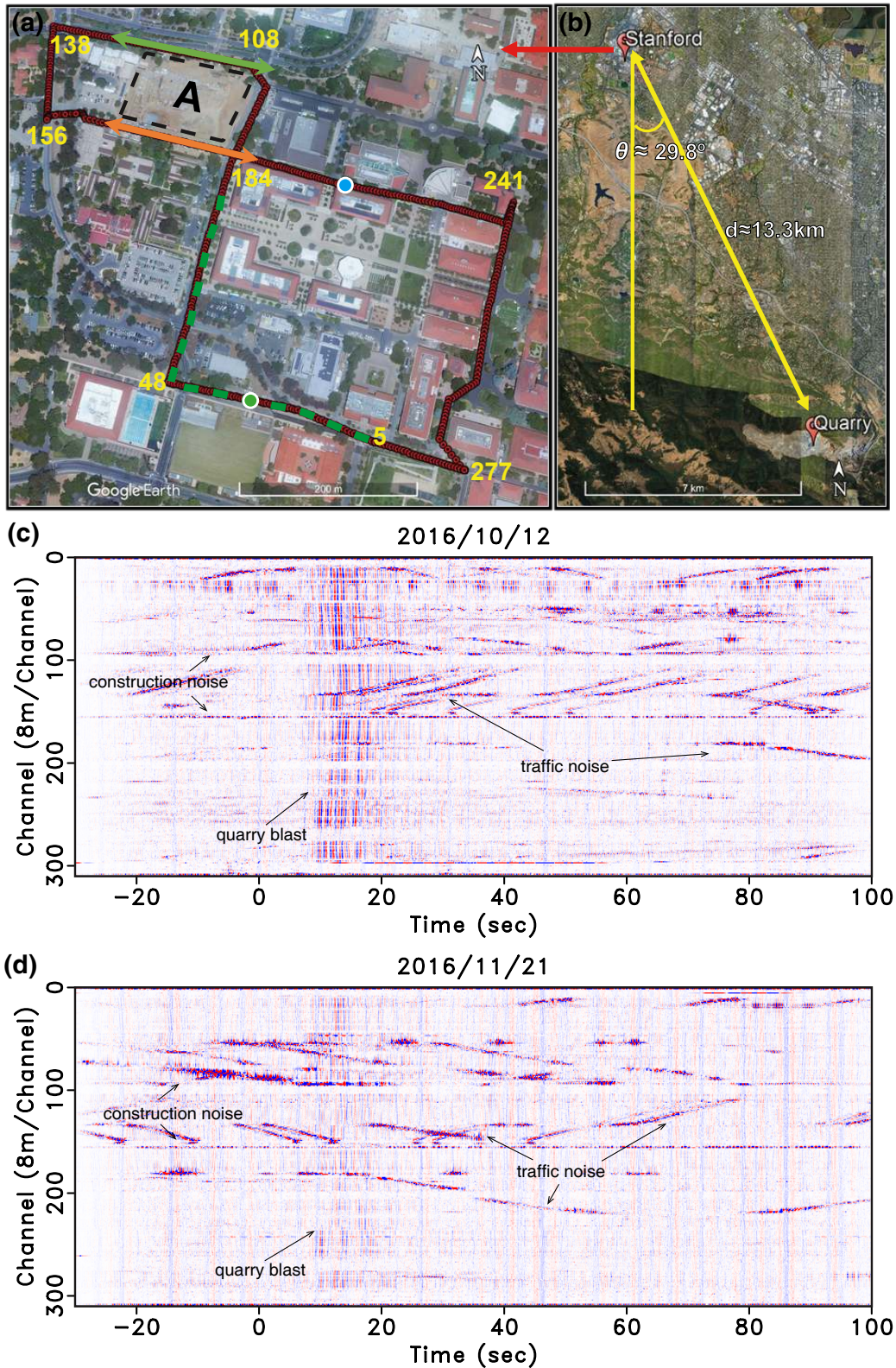
### 83 **3.1 Stanford Fiber Optic Seismic Observatory data acquisition**

84 The Stanford Fiber Optic Seismic Observatory (also called Stanford DAS Array) (Biondi  
85 et al., 2017) is one of the first DAS arrays to use existing telecommunication infrastruc-  
86 ture, and is the longest-running ultra-dense urban seismic study in the world. In this ex-  
87 periment, 2.5 kilometers of fiber-optic cable are deployed loosely in existing underground  
88 telecommunication conduits (typically 10–15 cm wide PVC pipes) under the Stanford  
89 University campus. Coupling between the fiber cable and the surrounding conduit re-  
90 lies only on gravity and friction. This experiment simulates DAS acquisition using dark  
91 fibers (the unused backup fiber-optic cables) that are commonly available in existing telecom-  
92 munication systems. Figure 1a shows the layout of the DAS array, which records data  
93 at a 25 Hz Nyquist frequency with 8.16 m channel spacing and 7.14m gauge length (Dean  
94 et al., 2017; Lindsey et al., 2017). Construction of a basement (labeled with "A" in Fig-  
95 ure 1a) began by its excavation on 7 November 2016.

### 103 **3.2 Quarry blasts data**

104 Lehigh Permanente Quarry is located 13.3 km away 29.9° southeast of the DAS ar-  
105 ray (Figure 1b). Figures 1c and 1d show the DAS recordings on 12 October 2016 18 :  
106 30 : 16.9 UTC and on 21 November 18 : 56 : 12.5 UTC, after applying a bandpass fil-  
107 ter from 0.25 to 2.5 Hz. The origin of the time axis denotes the blasting time provided  
108 by analysis of the data recorded by a USGS seismometer at the Jasper Ridge seismic sta-  
109 tion (JRSC) that is managed by the Berkeley Digital Seismic Network. The near ver-  
110 tical events originate from the quarry blasts, whereas strong dipping events are the di-  
111 rect impact of traffic on the fiber and the horizontal events are construction noise. We  
112 observe polarity flips around the corners of each pair of orthogonal segments of the DAS  
113 array (Figures 1c, 1d and Movie S1 in supporting information), which are caused by the  
114 angular sensitivity of DAS strain measurements (Lindsey et al., 2017). Table S1 in sup-  
115 porting information lists the time and the magnitude of 10 quarry blast events used for  
116 further analysis.

117 In the subsequent signal processing section, we aim to extract subsurface informa-  
118 tion based on far-field quarry blasts while minimizing the influence of near-field anthro-  
119 pogenic noise. Figures 2a and 2b zoom in on two blast signals after geometric polarity  
120 sign-correction (Biondi et al., 2017). Because of the strong surface wave energy originat-  
121 ing from the quarry blast and anthropogenic noise (mainly traffic and construction noise)



96 **Figure 1.** (a) Layout of the DAS array with the corner points labeled by the corresponding  
 97 channel numbers. The green dashed line represents the segment of DAS recording used for beam-  
 98 forming calculation in Figure 2. The green and orange arrows represent the segment of DAS  
 99 recording used in Figure 4. The green and blue dots are virtual sources used for seismic inter-  
 100 ferometry in Figures 4 and 5, respectively. Box A denotes the basement construction site. (b)  
 101 Location of the quarry relative to the DAS array. (c) and (d) Bandpassed DAS recordings on 12  
 102 October 2016 and 21 November 2016, respectively.

122 during the daytime, it is hard to identify any body wave in the records. Based on the  
 123 facts that the quarry blasts events propagate through the DAS array in a non-perpendicular  
 124 uniform direction and the arrival times of Rayleigh and Love waves are close, a combi-  
 125 nation of Rayleigh and Love waves are expected to be observed by the DAS array. The  
 126 blast vibration events reach the south portion of the array (channel 5) almost 0.7s ear-  
 127 lier than they reach the north portion (channel 138). This time lag matches the relative  
 128 distance and the average velocity between these two portions of the array, which is es-  
 129 timated in the next section. The blue lines overlaid on the profiles of Figures 2a and 2b  
 130 are the single-channel responses of channel 120 on two different days. Figures 2c and 2d  
 131 show their time-frequency spectrograms, respectively. Note that the main energy of the  
 132 two quarry blasts events arrives at the DAS array around 14s after the explosion. Their  
 133 dominant frequencies are approximately 1.2 Hz.

134 Beamforming based on multiple signal classification (MUSIC) (Zhang et al., 2019)  
 135 is applied on the southwest corner of the DAS array (indicated by green dashed line in  
 136 Figure 1a) within a small time window of 10-15s (labeled with the red dashed box in Fig-  
 137 ures 2a and 2b). Figures 2e, 2f and movie S2 in supporting information show the beam-  
 138 forming results for different days' data. Their peaks roughly indicate the wavefield prop-  
 139 agation direction and velocity, which support the assumption that the quarry blasts can  
 140 be seen as unidirectional plane wave sources. Although the quarry blasts signals recorded  
 141 at different times show certain similarity, their waveforms are complex and quite differ-  
 142 ent as shown by the blue lines in Figures 2a and 2b. The reasons for this difference may  
 143 lie in the randomness of explosive energy, excitation environment and the rugged earth  
 144 surface where the source is excited. Urban noise further contaminates the signals.

### 153 3.3 Signal processing

154 We propose a data processing workflow to reduce the impact of urban noise and  
 155 waveform differences. It starts with raw DAS records and results in cross-correlograms  
 156 between virtual sources and other channels, which are used for velocity estimation. The  
 157 workflow is the same for all quarry blasts.

158 **Bandpass, FK and median filter:** A Butterworth bandpass filter with cut-off  
 159 frequencies from 0.25 Hz to 2.5 Hz is applied to all quarry blast data. A narrowband  
 160 frequency-wavenumber(FK) filter is applied to remove the high frequency, large move-  
 161 out events, which are primarily generated by direct traffic impact or the equipment on  
 162 the construction site. Therefore, the parameters to control the FK filter are tuned daily  
 163 according to noise on that day. A sliding 2-D median filter is used to remove spike noise  
 164 for all the data.

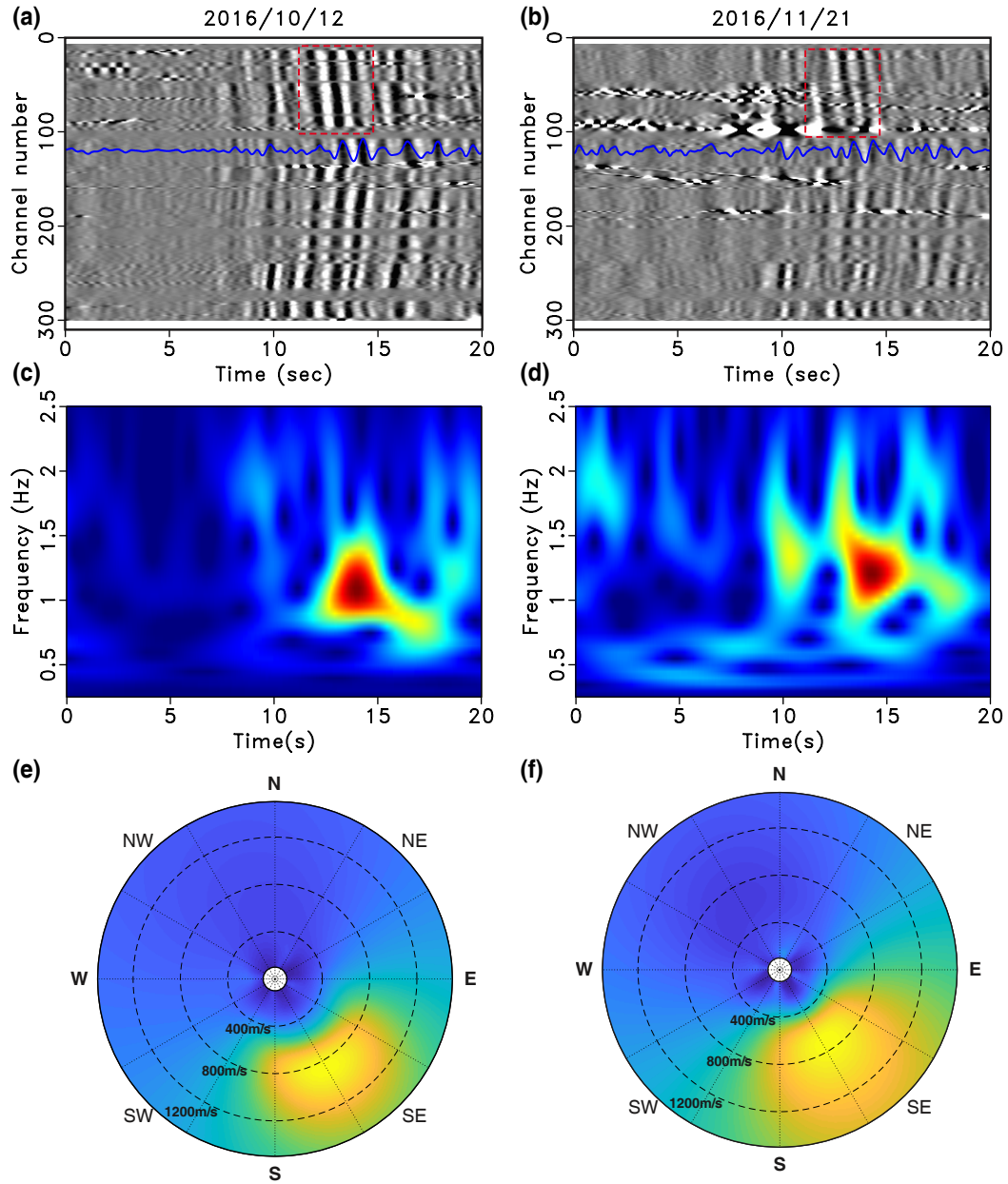
165 **Normalized cross-correlation:** The quarry sets off each blast with a different  
 166 source signature. We use normalized cross-correlation to eliminate the imprint of the source  
 167 signature. Under the assumption of far-field plane-wave propagation and uniform receiver  
 168 response, the signals  $U$  recorded at receivers  $A$  and  $B$  in the frequency domain can be  
 169 approximated by 1-D wave propagation as follows

$$170 \quad U(R_A, \omega) = S(R_S, \omega)e^{ikDis(R_A, R_S)}, \quad (1)$$

$$U(R_B, \omega) = S(R_S, \omega)e^{ikDis(R_B, R_S)}, \quad (2)$$

171 where  $S(R_S, \omega)$  is the source spectrum,  $k$  is the wavenumber,  $R_A$  and  $R_B$  are locations  
 172 of A and B,  $Dis(R_A, R_S)$  are the distance between  $R_A$  and  $R_S$ , respectively. The nor-  
 173 malized cross-correlation operator is defined as

$$C_N(R_A, R_B, \omega) = \frac{U(R_A, \omega)U^*(R_B, \omega)}{\langle\langle U(R_B, \omega)U^*(R_B, \omega) \rangle\rangle} \approx e^{ikDis(R_A, R_B)}, \quad (3)$$



145 **Figure 2.** Quarry blasts DAS data on (a) 12 October 2016 and (b) 21 November 2016. Both  
 146 plots (a) and (b) are after noise attenuation and polarity correction. Blue lines denote the signals  
 147 at channel 120. Plots (c) and (d) compare the time frequency spectrograms of these two days  
 148 data, which are calculated with the single channel shown with blue lines in plot (a) and (b), re-  
 149 spective. Plot (e) and (f) compare with the beamforming spectrum calculated with the data in  
 150 the red dashed box in (a) and (b), whose peaks indicate the wavefield direction of propagation  
 151 and its velocity. The channels used for beamforming are from 12-77, indicated by green dashed  
 152 line in Figure 1a.

174 where  $\ll \cdot \gg$  is a Gaussian smoothing operator. Equation 3 is an implementation  
 175 of deconvolution in the frequency domain, which can both remove the influence of the  
 176 source wavelet and improve the data resolution. More details of data processing results  
 177 can be found in supporting information Figures S1-S2.

## 178 4 Results

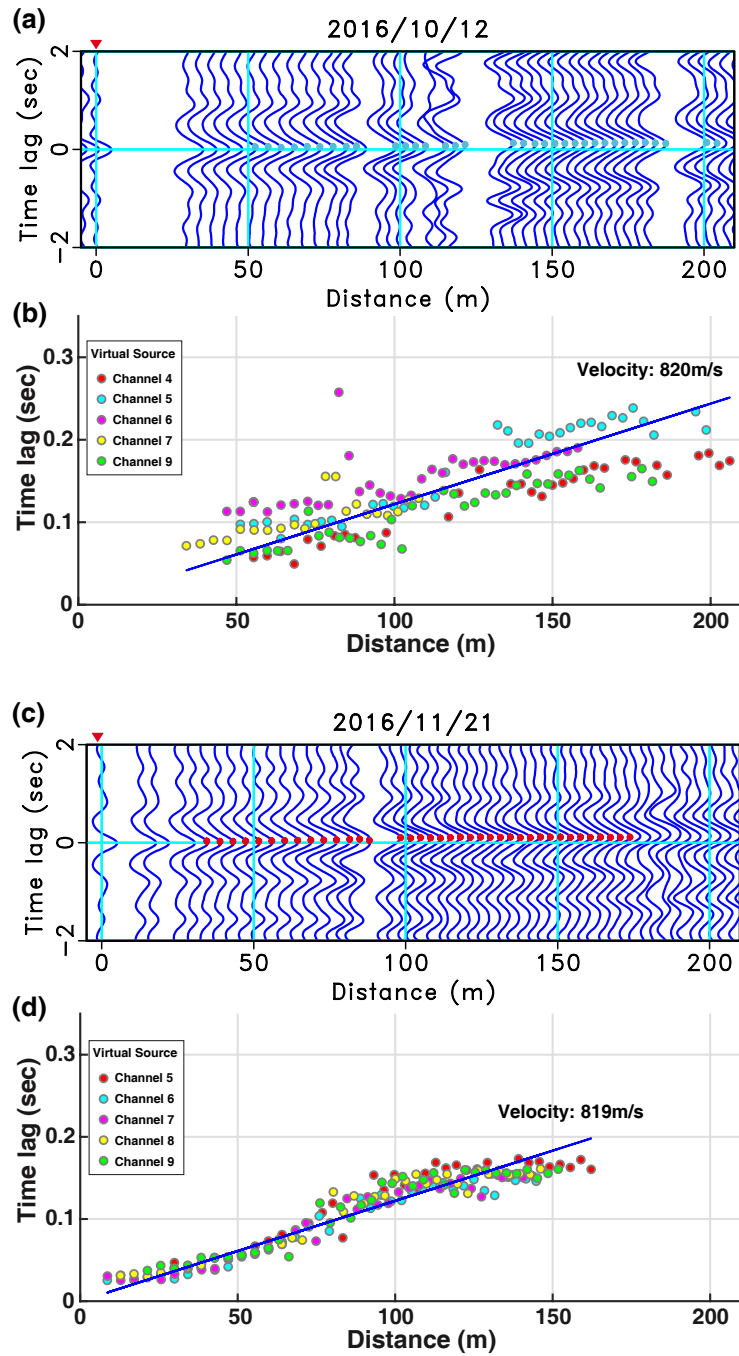
179 Using data recorded at channels away from the construction site, we first estab-  
 180 lish the baseline velocity of the site and demonstrate that DAS recordings, after urban  
 181 noise removal, can provide reliable velocity estimates. We select channels 5-48, use 5 chan-  
 182 nels near channel 5 as virtual sources, and calculate the normalized cross-correlograms.  
 183 Figure 3a shows one of these normalized cross-correlograms on 12 October 2016, whose  
 184 vertical axis represents the seismic time lag from virtual source to channels. The chan-  
 185 nels that are still contaminated by near-field noise after signal processing are omitted.  
 186 Figure 3b shows the picked travel-time lag along the distance between virtual source and  
 187 receiver, where the different colored dots denote the picks from different virtual sources.  
 188 Figures 3c and 3d are similar to Figures 3a and 3b but computed on 21 November 2016.  
 189 The surface seismic velocities are estimated by a least-squares linear regression of the  
 190 picked travel times on each day. After correction for the propagation angles obtained  
 191 from beamforming spectrums (as shown in Figures 2e and 2f), the measured velocities  
 192 on 10 different days show small variations over 3 months (Table S1 in supporting infor-  
 193 mation). The average velocity over 3 months is measured at 816 m/s and their coeffi-  
 194 cient of variation is 3.2%, with which the measurements at the construction site are bench-  
 195 marked.

205 When we focus on the segment of the array closer to the construction site, the ef-  
 206 fects of excavation on velocity are observed. We select two segments of the DAS record-  
 207 ings surrounding the construction site, one on the south edge (channels 170-184), and  
 208 the other on the north edge (channels 108-128). Figure 4 shows the normalized cross-  
 209 correlograms between channel 36 (the green dot in Figure 1a) and the two segments be-  
 210 fore and after the excavation. The measured arrival time shift in Figure 4 only depends  
 211 on the velocity within the boundaries of the DAS array. In Figures 4a and 4b, we ob-  
 212 serve that before construction started the surface wave arrivals show high spatial coherency  
 213 in both segments. Their picked arrival times (red solid line) with slight moveout across  
 214 the channels agree well with the computed arrival times (green dashed line) according  
 215 to the average velocity of 816 m/s. Figures 4c and 4d show the cross-correlograms two  
 216 weeks after excavation on both segments. In Figure 4c, the south channels maintain the  
 217 consistent arrival times at the reference velocity, indicating a stable subsurface environ-  
 218 ment between the two investigations (as expected because no excavation was performed  
 219 along this ray path). In Figure 4d, systematic time delays are observed on the north seg-  
 220 ment, which suggests that the subsurface velocity between the two segments was reduced  
 221 due to excavation of the basement.

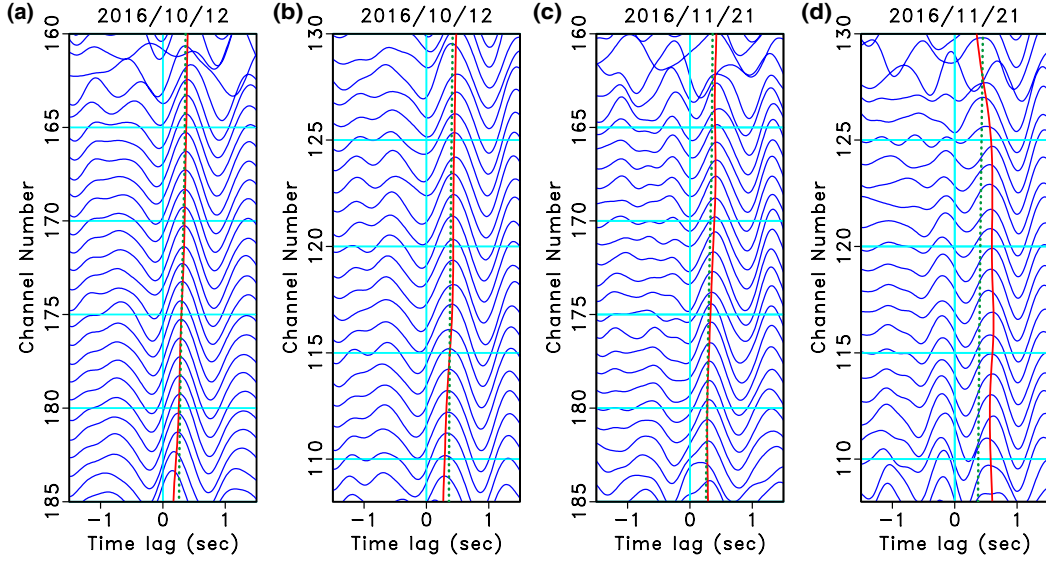
229 To investigate the spatial sensitivity of the passive DAS monitoring system, we ex-  
 230 tract surface wave velocities from channels 162-205, where the construction site is be-  
 231 tween channel 172 and 184. We use 3 channels near channel 205 as virtual sources to cal-  
 232 culate normalized cross-correlations. Figure 5a and 5b show one of the cross-correlograms  
 233 (channel 205 as virtual source) before and after the excavation, respectively. The black  
 234 lines denotes the picked travel time. Figure 5c displays the picked travel time versus dis-  
 235 tance (green dots: before excavation, red triangles: after excavation). The picked travel  
 236 times stay within the same clusters with similar linear trends at channels east and west  
 237 of the basement. At the basement, however, the cluster of red triangles deviates from  
 238 that of the green circles, indicating significant changes in velocity.

239 The yellow dashed and blue solid lines are the least-squares piecewise linear fit of  
 240 the red triangles and green dots of the three parts. As expected, at both the west (chan-





196 **Figure 3.** Five channels close to the channel 5 are used as virtual sources to calculate nor-  
 197 malized cross-correlograms with channels 5-48. Plot (a) shows the normalized cross-correlograms  
 198 on 12 October 2016. The channel used as virtual source (channel 5) is labeled with red triangle.  
 199 The x axis denote the distance between virtual source and each receiver. Cyan dots denote the  
 200 picked travel time lag. Plot (b) shows the picked time lag along the actual spatial distances from  
 201 all the normalized cross-correlograms. The dots with different color denote the time delay picked  
 202 with different virtual sources. Plot (c) and (d) are similar to (a) and (b), but computed on 21  
 203 November 2016. The marked surface seismic velocities are calculated by the slopes of the blue  
 204 lines.



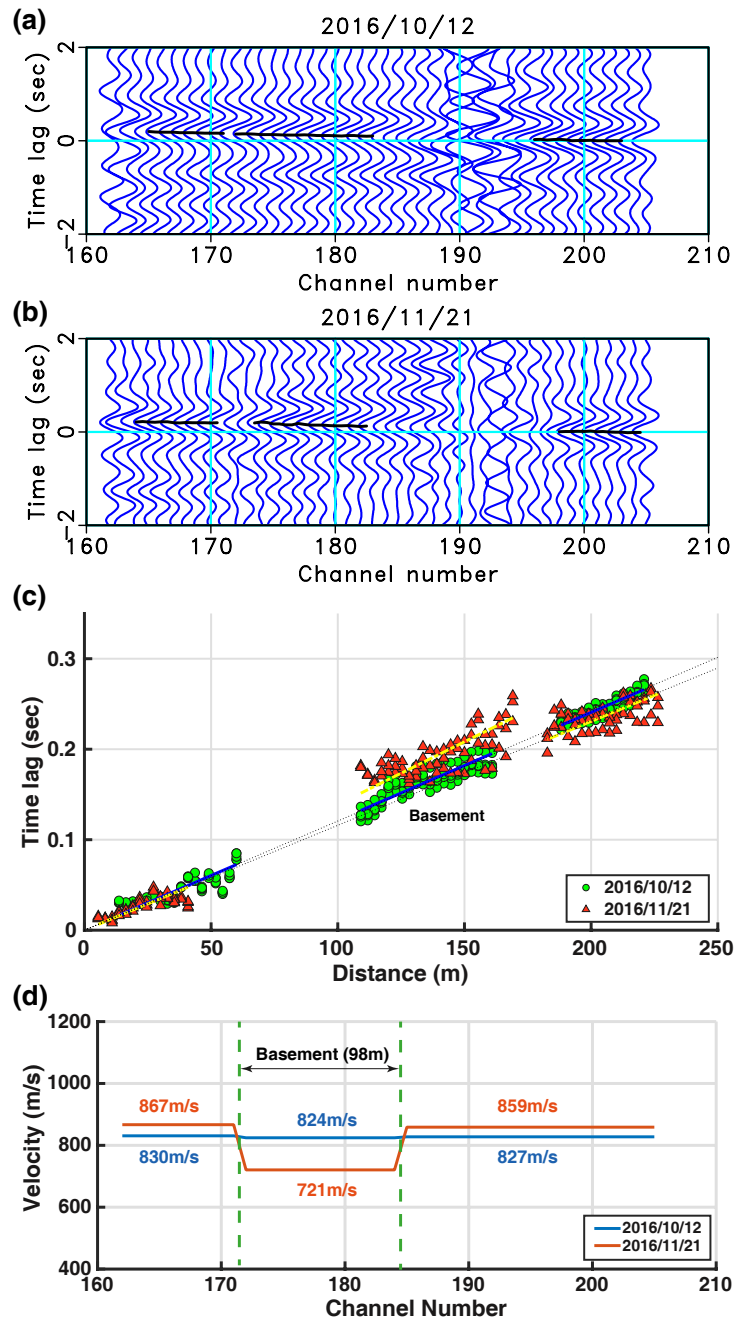
222 **Figure 4.** Plot (a) and (b) compare the normalized cross-correlograms between the virtual  
 223 source (channel 36) and the front channels 165-183 and the back channels 108-136 on 12 October  
 224 2016, respectively. The virtual source location is denoted by the green dot in Figure 1a. The  
 225 front and back channels are denoted by the orange and green lines in Figure 1a. Plot (c) and  
 226 (d) are similar to plots (a) and (b), but on 21 November 2016. The green dashed lines show the  
 227 calculated time lag according to the reference velocity,  $816\text{ m/s}$ . The red solid lines show the  
 228 picked time lag of the normalized cross-correlation.

241 nels 162-172) and east (channels 184-205) of the basement, the yellow and the blue lines  
 242 have very similar slopes. However, across the basement (channels 172-184) the yellow  
 243 line has a larger slope compared to the blue line, which indicates a lower subsurface ve-  
 244 locity. Figure 5d displays the estimated average velocities along the three segments. Com-  
 245 paring the velocities before and after excavation, it is obvious that the velocities to the  
 246 west and east of the basement are not significantly changed, whereas an apparent ve-  
 247 locity drop from  $824\text{ m/s}$  to  $721\text{ m/s}$  is observed at the basement. The relative veloc-  
 248 ity drop is 12.5%, nearly 4 times larger than the coefficient of variation 3.2% observed  
 249 at stable sections of the array. Therefore, we believe the velocity drop is statistically sig-  
 250 nificant, and caused by the excavation. This demonstrates the ability to detect changes  
 251 due to the excavation of a single building basement with unprecedented resolution for  
 252 a DAS-based urban seismic monitoring system.

## 260 5 Discussion

### 261 5.1 Observed velocity variations by DAS

262 Any monitoring system must strike an important balance between its sensitivity  
 263 in detecting changes and its accuracy in issuing an alarm. In this study, we show that  
 264 the velocity measured using a DAS array does vary in time and space. Factors leading  
 265 to the velocity variations are three-fold: random DAS measurement error, changes in noise  
 266 fields and source wavelet, and changes in subsurface geological conditions. Through care-  
 267 ful signal processing, we have reduced the effect of DAS measurement noise, changes in  
 268 noise fields and source wavelet, so as to improve our ability to isolate changes due to sub-  
 269 surface geological conditions.



253 **Figure 5.** (a) and (b): Normalized cross-correlograms on 12 October 2016 and 21 November  
 254 2016, respectively. The black lines denote the picked travel time for three segments along the  
 255 fiber cable. (c) Picked time lags on 12 October 2016 (Green circles) and 21 November 2016 (red  
 256 triangles) plotted against distance. The gap from 60-100 meters distance are caused by removing  
 257 the poor quality data around channel 193. The yellow dashed lines and the blue solid lines are  
 258 least-squares linear fits to the red triangles and the green circles respectively. (d) Average veloci-  
 259 ties measured in three segments before and after excavation with a channel interval of 8.16m.

Individual DAS channels have a lower signal-to-noise ratio (SNR) compared to conventional geophones in an ideal coupling condition (Lindsey et al., 2017; Yu et al., 2019). In this experiment, the fiber cable is loosely lying in an existing conduit, which further reduces the SNR. Moreover, DAS recordings in urban areas are severely contaminated by nearby construction and traffic noise. We observe a significant decrease in SNR after construction began, which reduces the sensitivity of velocity anomaly monitoring. The variations in measured velocity are quantified using data recorded in a geologically stable zone, and later used as baseline statistics to identify abnormal velocity variations caused by changes in subsurface geology.

With the Stanford DAS array, the measured velocity variation (12.5%) after excavation provides strong statistical confidence of detection of an anomaly. On the other hand, the 3.2% baseline variance suggests that small changes in subsurface velocity may not be identified by the Stanford DAS system, which may limit its applicability to identify the development of small cavities in urban environments. With newer DAS interrogators with smaller channel spacing and gauge length and higher frequency noise sources, there is in principle a chance to detect smaller velocity changes, such as sinkhole development. These baseline statistics and sensitivities vary with site conditions, acquisition parameters, and signal characteristics. Establishing baseline velocity measurements and uncertainty bounds is very important for quantitative urban monitoring.

## 5.2 Temporal resolution of DAS urban monitoring

Many of the passive seismic methods assume far-field and full azimuthal random sources with equipartitioning in energy (Roberts & Asten, 2008; Shapiro et al., 2005). However, urban ambient noise usually comes from fixed-location human activities that are often not perfectly random and isotropic (Bonnefoy-Claudet et al., 2006). When the sources are in close proximity to the array, longer recordings are used to increase the randomness and azimuthal coverage and reduce their susceptibility to near-field effects, particularly for the low SNR DAS recordings.

In this experiment, we make use of the repetitive quarry blasts as far-field, unidirectional sources to extract subsurface velocity based on much shorter recordings than would be required for an ambient noise approach. The temporal resolution of our experiment depends on the interval of the blasts, a few days in this case, which is sufficient for urban subsurface monitoring and alert. When an array is placed closer to a blast site that emits strong impulsive noises, abundant high-frequency signals may be recorded by DAS for higher spatial resolution subsurface monitoring.

## 6 Conclusions

Analysis of quarry blasts recorded by the Stanford Fiber Optic Seismic Observatory suggests that a surface DAS array in an existing communication infrastructure can be used for time-lapse monitoring of near-surface velocity changes. Compared to a 3.2% baseline velocity variation, a strong velocity decrease (12.5%) is observed after two weeks of a basement excavation. The high temporal resolution is achieved by making use of repetitive quarry blast signals and a careful data processing workflow to remove the near-field noise and to normalize the variations in the blasting conditions. Our study suggests that a DAS array deployed in existing communication infrastructure has a strong potential for high-resolution urban near-surface monitoring and urban geohazard risk management.

## Acknowledgments

We would like to thank Biondo Biondi for inspiring us with this study and providing the DAS data. We thank editor Gavin Hayes, Ariel Lellouch, and an anonymous reviewer

318 for their helpful comments. The cross-correlated DAS data used in this analysis are avail-  
 319 able at GitHub (<https://github.com/GeoGANGFANG/StanfordDASQuarryBlast>).  
 320 We acknowledge the EDB Petroleum Engineering Professorship and Cambridge Sens-  
 321 ing Pte Ltd for financial support. Yunyue Elita Li is funded by MOE Tier-1 Grant R-  
 322 302-000-182-114. Gang Fang is supported by National Natural Science Foundation of China  
 323 (41504109). We also thank the Madagascar open-source software.

## 324 References

- 325 Ajo-Franklin, J. B., Dou, S., Lindsey, N. J., Monga, I., Tracy, C., Robertson, M., ...  
 326 others (2019). Distributed acoustic sensing using dark fiber for near-surface  
 327 characterization and broadband seismic event detection. *Scientific reports*,  
 328 9(1), 1328.
- 329 Biondi, B., Martin, E., Cole, S., Karrenbach, M., & Lindsey, N. (2017). Earthquakes  
 330 analysis using data recorded by the stanford das array. *87th Annual Interna-*  
 331 *tional Meeting, SEG, Expanded Abstracts*, 2752-2756.
- 332 Bonnefoy-Claudet, S., Cotton, F., & Bard, P.-Y. (2006). The nature of noise wave-  
 333 field and its applications for site effects studies: A literature review. *Earth-*  
 334 *Science Reviews*, 79(3-4), 205–227.
- 335 Dahm, T., Heimann, S., & Bialowons, W. (2011). A seismological study of shallow  
 336 weak micro-earthquakes in the urban area of hamburg city, germany, and its  
 337 possible relation to salt dissolution. *Natural Hazards*, 58(3), 1111–1134.
- 338 Dean, T., Cuny, T., & Hartog, H. A. (2017). The effect of gauge length on axially  
 339 incident p-waves measured using fibre optic distributed vibration sensing. *Geo-*  
 340 *physical Prospecting*, 65(1), 84–193.
- 341 Díaz, J., Ruiz, M., Sánchez-Pastor, P. S., & Romero, P. (2017). Urban seismology:  
 342 On the origin of earth vibrations within a city. *Scientific reports*, 7(1), 15296.
- 343 Dou, S., Lindsey, N., Wagner, A. M., Daley, T. M., Freifeld, B., Robertson, M., ...  
 344 Ajo-Franklin, J. B. (2017). Distributed acoustic sensing for seismic monitoring  
 345 of the near surface: A traffic-noise interferometry case study. *Scientific reports*,  
 346 7(1), 11620.
- 347 Douglas, I. (2004). People induced geophysical risks and urban sustainability. *Wash-*  
 348 *ington DC American Geophysical Union Geophysical Monograph Series*, 150,  
 349 387–397.
- 350 Gutiérrez, F., Parise, M., De Waele, J., & Jourde, H. (2014). A review on natural  
 351 and human-induced geohazards and impacts in karst. *Earth-Science Reviews*,  
 352 138, 61–88.
- 353 Jousset, P., Reinsch, T., Ryberg, T., Blanck, H., Clarke, A., Aghayev, R., ...  
 354 Krawczyk, C. M. (2018). Dynamic strain determination using fibre-optic  
 355 cables allows imaging of seismological and structural features. *Nature commu-*  
 356 *nications*, 9(1), 2509.
- 357 Lindsey, N. J., Martin, E. R., Dreger, D. S., Freifeld, B., Cole, S., James, S. R., ...  
 358 Ajo-Franklin, J. B. (2017). Fiber-optic network observations of earthquake  
 359 wavefields. *Geophysical Research Letters*, 44(23), 11–792.
- 360 Martin, E. R., Huot, F., Ma, Y., Cieplicki, R., Cole, S., Karrenbach, M., & Biondi,  
 361 B. L. (2018). A seismic shift in scalable acquisition demands new processing:  
 362 Fiber-optic seismic signal retrieval in urban areas with unsupervised learning  
 363 for coherent noise removal. *IEEE Signal Processing Magazine*, 35(2), 31–40.
- 364 Parker, T., Shatalin, S., & Farhadiroushan, M. (2014). Distributed acoustic sensing—  
 365 a new tool for seismic applications. *first break*, 32(2), 61–69.
- 366 Renalier, F., Jongmans, D., Campillo, M., & Bard, P.-Y. (2010). Shear wave ve-  
 367 locity imaging of the avignonet landslide (france) using ambient noise cross  
 368 correlation. *Journal of Geophysical Research: Earth Surface*, 115(F3).
- 369 Roberts, J., & Asten, M. (2008). A study of near source effects in array-based (spac)  
 370 microtremor surveys. *Geophysical Journal International*, 174(1), 159–177.

- 371 Schenato, L., Palmieri, L., Camporese, M., Bersan, S., Cola, S., Pasuto, A., ... Si-  
372 monini, P. (2017). Distributed optical fibre sensing for early detection of  
373 shallow landslides triggering. *Scientific reports*, 7(1), 14686.
- 374 Shapiro, N. M., Campillo, M., Stehly, L., & Ritzwoller, M. H. (2005). High-  
375 resolution surface-wave tomography from ambient seismic noise. *Science*,  
376 307(5715), 1615–1618.
- 377 Spica, Z., Perton, M., Martin, E. R., Biondi, B., & Beroza, G. (2019). Urban seismic  
378 site characterization by fiber-optic seismology. *EarthArXiv*.
- 379 Tran, K. T., & Sperry, J. (2018). Application of 2d full-waveform tomography on  
380 land-streamer data for assessment of roadway subsidence. *Geophysics*, 83(3),  
381 EN1–EN11.
- 382 Willis, M. E., Barfoot, D., Ellmauthaler, A., Wu, X., Barrios, O., Erdemir, C., ...  
383 Quinn, D. (2016). Quantitative quality of distributed acoustic sensing vertical  
384 seismic profile data. *The Leading Edge*, 35(7), 605–609.
- 385 Yu, C., Zhan, Z., Lindsey, N. J., Ajo-Franklin, J. B., & Robertson, M. (2019). The  
386 potential of das in teleseismic studies: Insights from the goldstone experiment.  
387 *Geophysical Research Letters*, 46(3), 1320–1328.
- 388 Zhang, Y., Li, Y. E., Zhang, H., & Ku, T. (2019). Near-surface site investigation by  
389 seismic interferometry using urban traffic noise in singapore. *Geophysics*, 84(2),  
390 B169–B180.